Credit: Giovanola
Steel linings of the surge shaft of Fionnay (Louvie) in Giovanola's workshops

SAFETY ASSESSMENT OF AGEING STEEL-LINED PRESSURE TUNNELS AND SHAFTS

Dr Alexandre Pachoud[(a)], Reynald Berthod[(b)], Eric Papilloud[(c)], Dr Oliver Chène[(c)]

(a) SFOE (formerly Gruner Stucky SA): alexandre.pachoud@bfe.admin.ch
(b) Gruner Stucky SA: reynald.berthod@gruner.ch
(c) ALPIQ: eric.papillou@alpiq.ch; olivier.chene@alpiq.ch

EWG Penstocks, Pressure Shafts & Pressure Tunnels
Milan, Italy, November 3-4, 2022

FOREWORD

- This work was conducted by Gruner Stucky SA (former affiliation of the presenting author at the time when the study was performed, now working at the Swiss Federal Office of Energy SFOE) in collaboration with ALPIQ

- The technical outcomes presented hereinafter are the results of the engineering studies performed under the above scope. Those studies were not supervised by SFOE and should not represent a SFOE's position on the matter

INTRODUCTION

- **Framework**: rehabilitation project of Grande Dixence (GD) waterways, built from 1950 to 1965
- **Scope**: safety assessment of steel-lined parts of the scheme (both HHPs) against internal pressure and external loadings, including:
  a. stresses in lining
  b. stresses transmitted to rock;
  c. buckling resistance *(not presented herein)*
- **Objective**: assessment of the *effective* safety with respect to the working stress criterion assuming load sharing, and verification whether original design safety targets and assumptions are met (when known)

  Results are compared with C.E.C.T. (1980) recommendations for information and comparative evaluation purposes

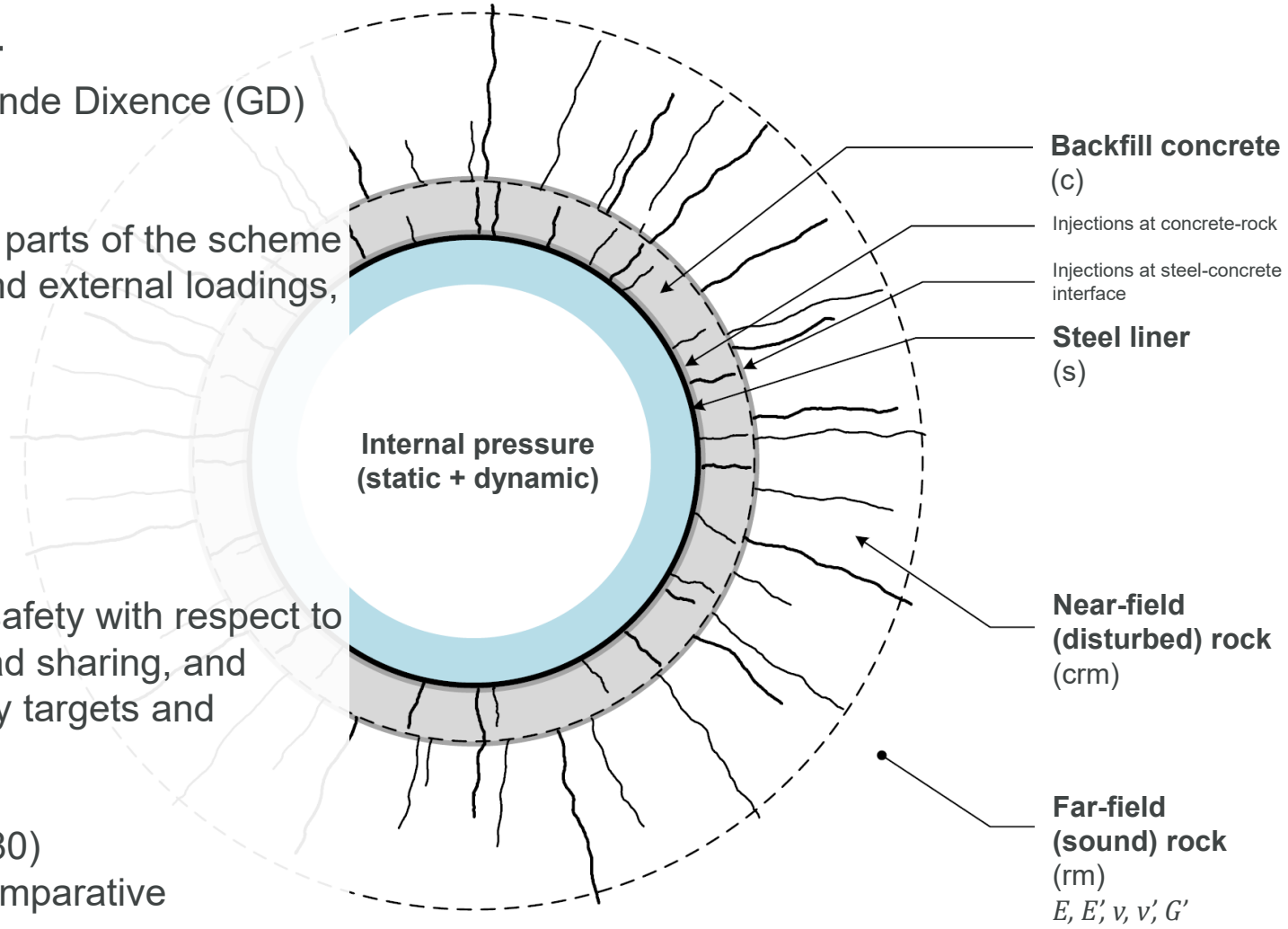

INTRODUCTION

- **A global approach of fitness-for-service**: in parallel, inspections and testing (incl. Non-Destructive Testing – NDT) have been performed on selected areas, combined with fracture mechanics assessment in the frame of a fitness-for-service approaches

- The study presented herein constitutes the "**reverse engineering**" part of this global approach, i.e., the review of the initial design and the global modeling of the behaviour of the steel-lined systems

- The content of this presentation is therefore only one element of a broader fitness-for-service approach, combining macroscopic analyses and detailed studies of special parts

THE GRANDE DIXENCE POWER SCHEME: THE CASCADE OF FIONNAY AND NENDAZ HPPS

Complete rehabilitation of Nendaz penstock (Condémines)

Steel-lined gallery stretch and surge shaft (Péroua)

Steel linings at intake of Fionnay Reservoir

Steel-lined gallery stretch and surge shaft (Louvie)

Fionnay inclined shaft

Steel linings at GD Dam

Nendaz vertical shaft

Nendaz inclined shaft

Fionnay HPP manifold

Nendaz HPP manifold

390 MW
~1'000 mWC (static pressure)
~1'100 mWC (design pressure)

290 MW
~870 mWC (static pressure)
~960 mWC (design pressure)

Grande Dixence SA. Technical documentation, 2015
http://www.grande-dixence.ch/docs/default-source/documentation/brochure-technique/Grande-Dixence-technical-documentation-2.pdf?sfvrsn=7 (last accessed on 30.09.2022)

DATA

Input	Sources
General scheme data	General and detailed project drawings (elevations, length of waterways, slopes, static head, etc.)
Steel liners	Project detailed drawings and material testing from Steel Works Contractors (diameters, thicknesses, stiffeners, yield stresses, ultimate tensile strengths, special parts) Updates and/or complementary information from correspondence between the Owner and the Steel Works Contractors Comparisons with posterior Owner's synthesis drawings or projects, when available
Geology and rock mass	Project geological drawings and technical documentation (investigations, geomechanical models, etc.) Recent expert geologists' technical notes and syntheses for the Owner and its Engineer(s)
Injections	Project detailed drawings (presence of injection holes, injection patterns and sequences, injection pressures when available), contracts with Steel Works Contractors
Gap	Thermal shrinkage from literature, accounting for injection sequences (see previous) and (rare) reports of air temperature during the works Permanent displacements estimated based on reproduction of pressure tests (availability of some project technical reports)
Internal pressure	General scheme data and pursuant to C.E.C.T. (1980) for dynamic pressure profiles
Criteria for rock participation	Estimation of rock cover (*swisstopo* and project drawings), evaluation of local configurations in the vicinity of underground openings (access galleries, caverns, etc.) Basic and conservative hypotheses on in situ stresses

METHODOLOGY – SAFETY ASSESSMENT

- Safety against internal pressure is assessed based on the working stress criterion, i.e.

$$\sigma_{eq}^{s} \leq \frac{f_y}{\mathrm{SF}}$$

where f_y is the steel yield stress; SF the safety factor and σ_{eq}^{s} is the equivalent Von Mises stress

- **Objective**: assessment of the effective safety assuming load sharing where applicable, and verification whether original design safety targets and assumptions are met (when known)

- Results are compared with the recommendations of the C.E.C.T. for info and comparative evaluation

METHODOLOGY – BASIS OF EVALUATION

- General formulation (thin-walled pipes) of the original design to determine shell's initial thickness t_i :

$$t_i = \frac{p_{i,d} \cdot D_i}{2 \cdot C_w \cdot C_o \cdot \sigma_{allow}} + s_c$$

  - C_w: weld factor (max 1.0)
  - C_o: overburden factor (may be lower than 1.0 in case of low overburden)
  - σ_{allow}: allowable stress (portion of yield stress f_y), also accounting for load sharing
  - s_c: corrosion allowance (generally 1-2 mm added to the first term rounded up to the nearest mm)

- At the time of construction (50-60s), there was no defined standards: significant (lump value on a given stretch) or no load sharing was assumed based on the location of the tunnel or shaft (overburden, rock quality, etc.), from interpretation of pressure tests and experts' analyses

- The formulation for each part was in general retrieved from project documentation (contracts with Steel Works Contractors, design drawings, etc.) but was not always available for comparison

- Load sharing assumptions (when applicable), depending on surrounding rock types, were also available in contracts or other technical reports

METHODOLOGY – ORIGINAL ADDITIONS TO THE «TRADITIONAL» LOAD SHARING EQUATIONS

- Consideration of rock anisotropy (where applicable) and its influence on the maximum stress in the steel liner (empirical correction from literature)
- Consideration of corrosion of the pipes if applicable (or under the form of parametric study)
- Quantitative attempt to estimate of permanent displacements (induced only by the static component of the internal pressure) in concrete-rock (e.g., yielding, creeping, settlements, etc.) based on the pressure tests' results available
- Consideration of the effect of injections (both in terms of gap and "pre-stress" pressure)

METHODOLOGY – «TRADITIONAL» LOAD SHARING EQUATIONS

- Pressure p_c transmitted to the concrete-rock system (isotropic rock), from deformation compatibility:

$$p_c = \max\left\{ \frac{\frac{1+\nu_s}{E_s}\frac{r_i+t_i}{(r_i+t_i)^2-r_i^2}\left[(1-2\nu_s)p_i r_i^2 + p_i r_i^2\right] - \Delta r_0}{\frac{1+\nu_s}{E_s}\frac{r_i+t_i}{(r_i+t_i)^2-r_i^2}\left[(1-2\nu_s)(r_i+t_i)^2 + r_i^2\right] + r_c\left[\frac{1-\nu_c^2}{E_c}\ln\left(\frac{r_{crm}}{r_c}\right) + \frac{1-\nu_{crm}^2}{E_{crm}}\ln\left(\frac{r_{rm}}{r_{crm}}\right) + \frac{1+\nu}{E'}\right]} ; 0 \right\}$$

(cracked) backfill concrete — disturbed (cracked) near-field rock — far-field (sound) rock

- Empirical correction for anisotropic (transversal isotropy – defined by 5 independent elastic parameters) rock mass behaviour (estimate of the maximum hoop stress in the steel liner):

$$p_c = \max\left\{ \frac{\frac{1+\nu_s}{E_s}\frac{r_i+t_i}{(r_i+t_i)^2-r_i^2}\left[(1-2\nu_s)p_i r_i^2 + p_i r_i^2\right] - \Delta r_0}{\frac{1+\nu_s}{E_s}\frac{r_i+t_i}{(r_i+t_i)^2-r_i^2}\left[(1-2\nu_s)(r_i+t_i)^2 + r_i^2\right] + r_c\left[\frac{1-\nu_c^2}{E_c}\ln\left(\frac{r_{crm}}{r_c}\right) + \frac{1-\nu_{crm}^2}{E_{crm}}\ln\left(\frac{r_{rm}}{r_{crm}}\right) + \underbrace{\prod_{i=1}^{3} X_i^{\alpha_i}}_{\left(\frac{E}{E'}\right)^{-0.65}\left(\frac{G}{G'}\right)^{0.50}\left(\frac{1+\nu}{1+\nu'}\right)^{-0.56}} \cdot \frac{1+\nu}{E'}\right]} ; 0 \right\}$$

Pachoud & Schleiss (2016)

METHODOLOGY – ORIGINAL ADDITIONS TO THE «TRADITIONAL» LOAD SHARING EQUATIONS

- Explicit separation between the static and dynamic parts of the design pressure:

$$p_{i,dim} = p_{i,stat} + p_{i,dyn}$$

$$\sigma_t^s = \sigma_{t,stat}^s + \sigma_{t,dyn}^s$$

- Consideration of a factor $f_{\%}$ (from 0 to 1) accounting for permanent displacements (yielding, creeping, settlements, etc.):

$$\sigma_{t,stat}^s = \frac{1}{(r_i + t_i)^2 - r_i^2}\left[r_i^2 p_{i,stat} - (r_i + t_i)^2 (f_{\%} p_{c,stat}) - (r_i + t_i)^2 \left(f_{\%} p_{c,stat} - p_{i,stat}\right)\right]$$

$$u_{r,stat}^s (r_i + t_i) = \frac{1 + \nu_s}{E_s} \frac{r_i + t_i}{(r_i + t_i)^2 - r_i^2}\left[(1 - 2\nu_s)(p_{i,stat} r_i^2 - f_{\%} p_{c,stat} (r_i + t_i)^2) + (p_{i,stat} - f_{\%} p_{c,stat}) r_i^2\right]$$

METHODOLOGY – ORIGINAL ADDITIONS TO THE «TRADITIONAL» LOAD SHARING EQUATIONS

- Consideration of the injection pressure p_{inj} with a factor $f_{\%,inj}$ (from 0 to 1) characterising its residual value:

$$u_r^{s,inj}(r_i + t_i) = -\frac{1+\nu_s}{E_s}\frac{r_i + t_i}{(r_i + t_i)^2 - r_i^2}\left[(1-2\nu_s) f_{\%,inj} p_{inj} (r_i + t_i)^2 + f_{\%,inj} p_{inj} r_i^2\right]$$

Different approach than in Pachoud et al. (2018) where injections were considered as a negative displacement; proposition of correction in a technical paper under preparation

$$p_{c,stat} = \max\left\{\frac{\frac{1+\nu_s}{E_s}\frac{r_i + t_i}{(r_i + t_i)^2 - r_i^2}\left[(1-2\nu_s) p_{i,stat} r_i^2 + p_{i,stat} r_i^2\right] - \Delta r_0}{\frac{1+\nu_s}{E_s}\frac{r_i + t_i}{(r_i + t_i)^2 - r_i^2}\left[(1-2\nu_s)(r_i + t_i)^2 + r_i^2\right] + r_c\left[\frac{1-\nu_c^2}{E_c}\ln\left(\frac{r_{crm}}{r_c}\right) + \frac{1-\nu_{crm}^2}{E_{crm}}\ln\left(\frac{r_{rm}}{r_{crm}}\right) + \prod_{i=1}^{3} X_i^{\alpha_i} \cdot \frac{1+\nu}{E'}\right]} + f_{\%,inj} p_{inj}; 0\right\}$$

- Then the total gap between the steel liner and the backfill concrete is obtained as follows and $p_{c,dyn}$ is calculated:

$$\boldsymbol{\Delta r_{0,res}} = \max\{[\Delta r_0 - u_{r,stat}^{s}(r_i + t_i) + u_r^{s,inj}(r_i + t_i)]; 0\}$$

$$p_{c,dyn} = \max\left\{\frac{\frac{1+\nu_s}{E_s}\frac{r_i + t_i}{(r_i + t_i)^2 - r_i^2}\left[(1-2\nu_s) p_{i,dyn} r_i^2 + p_{i,dyn} r_i^2\right] - \boldsymbol{\Delta r_{0,res}}}{\frac{1+\nu_s}{E_s}\frac{r_i + t_i}{(r_i + t_i)^2 - r_i^2}\left[(1-2\nu_s)(r_i + t_i)^2 + r_i^2\right] + r_c\left[\frac{1-\nu_c^2}{E_c}\ln\left(\frac{r_{crm}}{r_c}\right) + \frac{1-\nu_{crm}^2}{E_{crm}}\ln\left(\frac{r_{rm}}{r_{crm}}\right) + \prod_{i=1}^{3} X_i^{\alpha_i} \cdot \frac{1+\nu}{E'}\right]}, 0\right\}$$

METHODOLOGY – ORIGINAL ADDITIONS TO THE «TRADITIONAL» LOAD SHARING EQUATIONS

- The factor $f_{\%}$ accounting for permanent displacements can be interpreted as a permanent gap $\Delta r_{f\%}$ as:

$$f_{\%}p_{c,stat} = \frac{\frac{1+\nu_s}{E_s}\frac{r_i+t_i}{(r_i+t_i)^2-r_i^2}\left[(1-2\nu_s)p_{i,stat}r_i^2 + p_{i,stat}r_i^2\right] - \Delta r_0 - \boldsymbol{\Delta r_{f\%}}}{\frac{1+\nu_s}{E_s}\frac{r_i+t_i}{(r_i+t_i)^2-r_i^2}\left[(1-2\nu_s)(r_i+t_i)^2 + r_i^2\right] + r_c\left[\frac{1-\nu_c^2}{E_c}\ln\left(\frac{r_{crm}}{r_c}\right) + \frac{1-\nu_{crm}^2}{E_{crm}}\ln\left(\frac{r_{rm}}{r_{crm}}\right) + \prod_{i=1}^{3} X_i^{\alpha_i}\cdot\frac{1+\nu}{E'}\right]} + f_{\%,inj}p_{inj}$$

- By reorganising the above expression, one obtains the following formulation for the permanent displacements (set to zero if negative):

$$\boldsymbol{\Delta r_{f\%}} = u_{r,stat}^{s}(r_i+t_i) - u_r^{s,inj}(r_i+t_i) - (f_{\%}p_{c,stat} - f_{\%,inj}p_{inj})r_c\left[\frac{1-\nu_c^2}{E_c}\ln\left(\frac{r_{crm}}{r_c}\right) + \frac{1-\nu_{crm}^2}{E_{crm}}\ln\left(\frac{r_{rm}}{r_{crm}}\right) + \prod_{i=1}^{3} X_i^{\alpha_i}\cdot\frac{1+\nu}{E'}\right] - \Delta r_0$$

which can then be used to estimate the part of the dynamic pressure withstood by the concrete-rock system

METHODOLOGY – ORIGINAL ADDITIONS TO THE «TRADITIONAL» LOAD SHARING EQUATIONS

- Finally, potential corrosion (e.g., loss of thickness at the external fibre $\Delta t_{i,ext}$) can also be accounted for as follows, ensuring full continuity of the equations:

$$p_{c,stat} = \max\left\{\frac{\frac{1+\nu_s}{E_s}\frac{(r_i+t_i-\Delta t_{i,ext})}{(r_i+t_i-\Delta t_{i,ext})^2-r_i^2}\left[(2-2\nu_s)p_{i,stat}r_i^2\right]-(\Delta r_0+\Delta r_{f\%}+\Delta t_{i,ext})}{\frac{1+\nu_s}{E_s}\frac{(r_i+t_i-\Delta t_{i,ext})}{(r_i+t_i-\Delta t_{i,ext})^2-r_i^2}\left[(1-2\nu_s)(r_i+t_i-\Delta t_{i,ext})^2+r_i^2\right]+r_c\left[\frac{1-\nu_c^2}{E_c}\ln\left(\frac{r_{crm}}{r_c}\right)+\frac{1-\nu_{crm}^2}{E_{crm}}\ln\left(\frac{r_{rm}}{r_{crm}}\right)+\prod_{i=1}^{3}X_i^{\alpha_i}\cdot\frac{1+\nu}{E'}\right]}+f_{\%,inj}p_{inj},0\right\}$$

$$\boldsymbol{\Delta r_{0,res}} = \max\{[\Delta r_0+\Delta r_{f\%}+\Delta t_{i,ext}-u_{r,stat}^{s}(r_i+t_i-\Delta t_{i,ext})+u_r^{s,inj}(r_i+t_i-\Delta t_{i,ext})];0\}$$

$$p_{c,dyn} = \max\left\{\frac{\frac{1+\nu_s}{E_s}\frac{(r_i+t_i-\Delta t_{i,ext})}{(r_i+t_i-\Delta t_{i,ext})^2-r_i^2}\left[(2-2\nu_s)p_{i,dyn}r_i^2\right]-\boldsymbol{\Delta r_{0,res}}}{\frac{1+\nu_s}{E_s}\frac{(r_i+t_i-\Delta t_{i,ext})}{(r_i+t_i-\Delta t_{i,ext})^2-r_i^2}\left[(1-2\nu_s)(r_i+t_i-\Delta t_{i,ext})^2+r_i^2\right]+r_c\left[\frac{1-\nu_c^2}{E_c}\ln\left(\frac{r_{crm}}{r_c}\right)+\frac{1-\nu_{crm}^2}{E_{crm}}\ln\left(\frac{r_{rm}}{r_{crm}}\right)+\prod_{i=1}^{3}X_i^{\alpha_i}\cdot\frac{1+\nu}{E'}\right]},0\right\}$$

METHODOLOGY – ORIGINAL ADDITIONS TO THE «TRADITIONAL» LOAD SHARING EQUATIONS

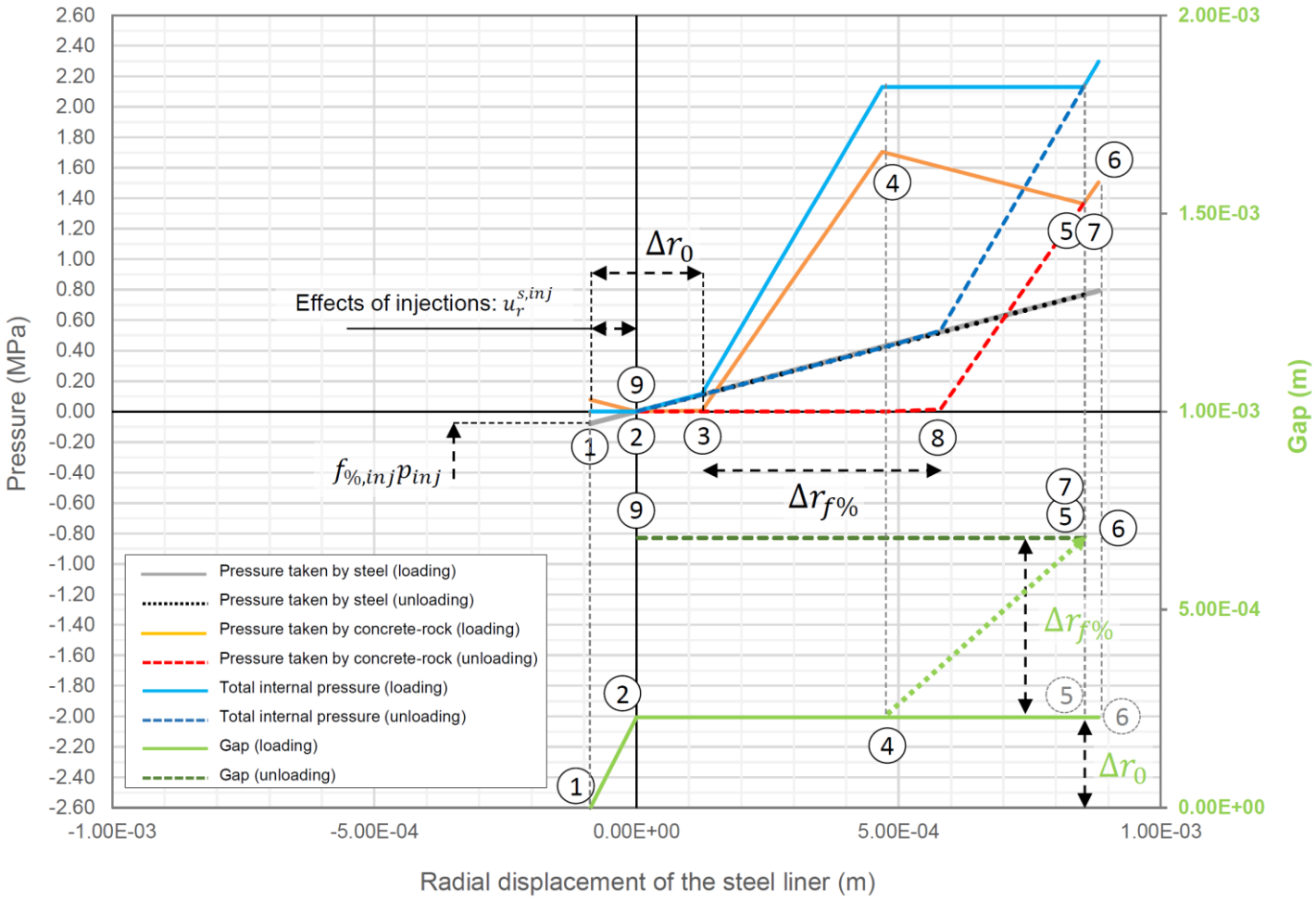

(1) Initial state, injection pressure applies to steel liner and concrete-rock system ($f_{\%,inj} = 20\%$ in example). The radial displacement of the steel liner is negative.

(2) Thermal loading on steel liner at first filling (zero pressure). The steel lining is subjected to a thermal shrinkage of Δr_0, herein greater than the displacement induced by injection pressure. There is still no internal pressure, a gap is initiated.

(3) The steel liner withstands alone internal pressure until the radial displacement is equivalent to the gap, reduced by injections. When the steel liner comes into contact with concrete, the **concrete-rock system starts to participate**.

(4) Internal pressure reaches maximum static pressure.

(5) Permanent displacements occur in concrete-rock system ($f_{\%} = 80\%$). In the model, the gap is not yet increased by $\Delta r_{f\%}$ (see number 5 in grey). The permanent displacements are comprised in the "creeping" factor $f_{\%}$. This is only due to the sequence of implementation of the equations. Shall $f_{\%}$ be applied progressively under the form of a permanent displacement once maximum static pressure is applied, the green dashed line would be followed. Sequences 5-6 are outlined on the plot as above described, which is more intuitive (in black on the plot).

(6) The dynamic part of the pressure is applied. The latter does not induce additional permanent displacements.

(7) Unloading of dynamic pressure. From this point, $\Delta r_{f\%}$ is added to the gap before the unloading of the static pressure (see remark at number 5).

(8) Unloading until the steel liner does not sollicitate concrete-rock system.

(9) Complete unloading. The gap (thermal shrinkage + permanent displacements) is greater than the effects of the injections. The steel liner is not loaded without internal pressure.

REPRODUCTION OF PRESSURE TESTS: THE FIONNAY INCLINED SHAFT

Mise en pression du 30 III 1957

heure	pression	eau introd. - pertes extérieures	compression de l'eau	pertes du puits	dilatation du puits litres	
minutes	kg/cm²	△litres	△litres	△litres	△	Σ
8.00	0				0	0
03	1,0	env. 720	-358	-10	352	352
12	3,2	951	-787	-30	134	486
21	5,2	945	-716	-32	197	683
30	7,1	945	-682	-33	230	913
40	9,0	944	-682	-40	222	1135
49	10,8	944	-645	-38	261	1396
9.00	12,6	933	-645	-48	240	1636
09	14,4	938	-645	-40	253	1889
18	16,4	938	-716	-43	179	2068
29	18,4	925	-716	-55	154	2222
44	20,2	905	-645	-76	184	2406
55	21,9	906	-608	-60	238	2644
10.08	23,7	899	-645	-74	180	2824
52	24,8	890	-394	-277	219	3043
11.35	26,1	889	-466	-309	114	3157
12.19	27,2	885	-394	-360	131	3288
13.03	28,2	885	-358	-400	127	3415
48	29,1	884	-322	-447	115	3530
14.32	30,1	884	-358	-450	46	3576
15.18	30,8	878	-256	-546	76	3652
56	31,0	710	- 72	-505	133	3785
totaux:		18798	-11110	-3903	3785	

Project documentation

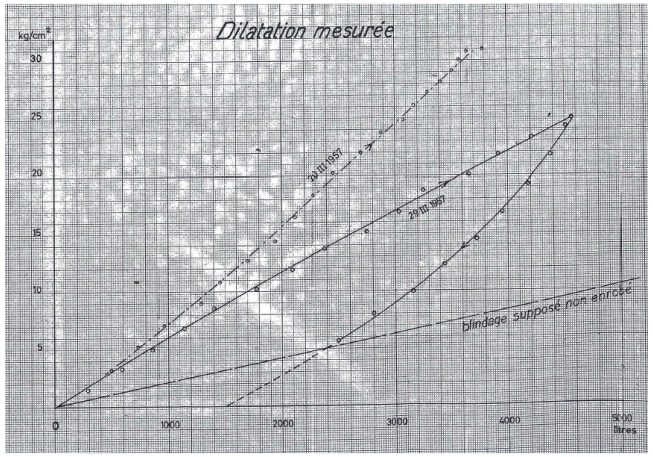

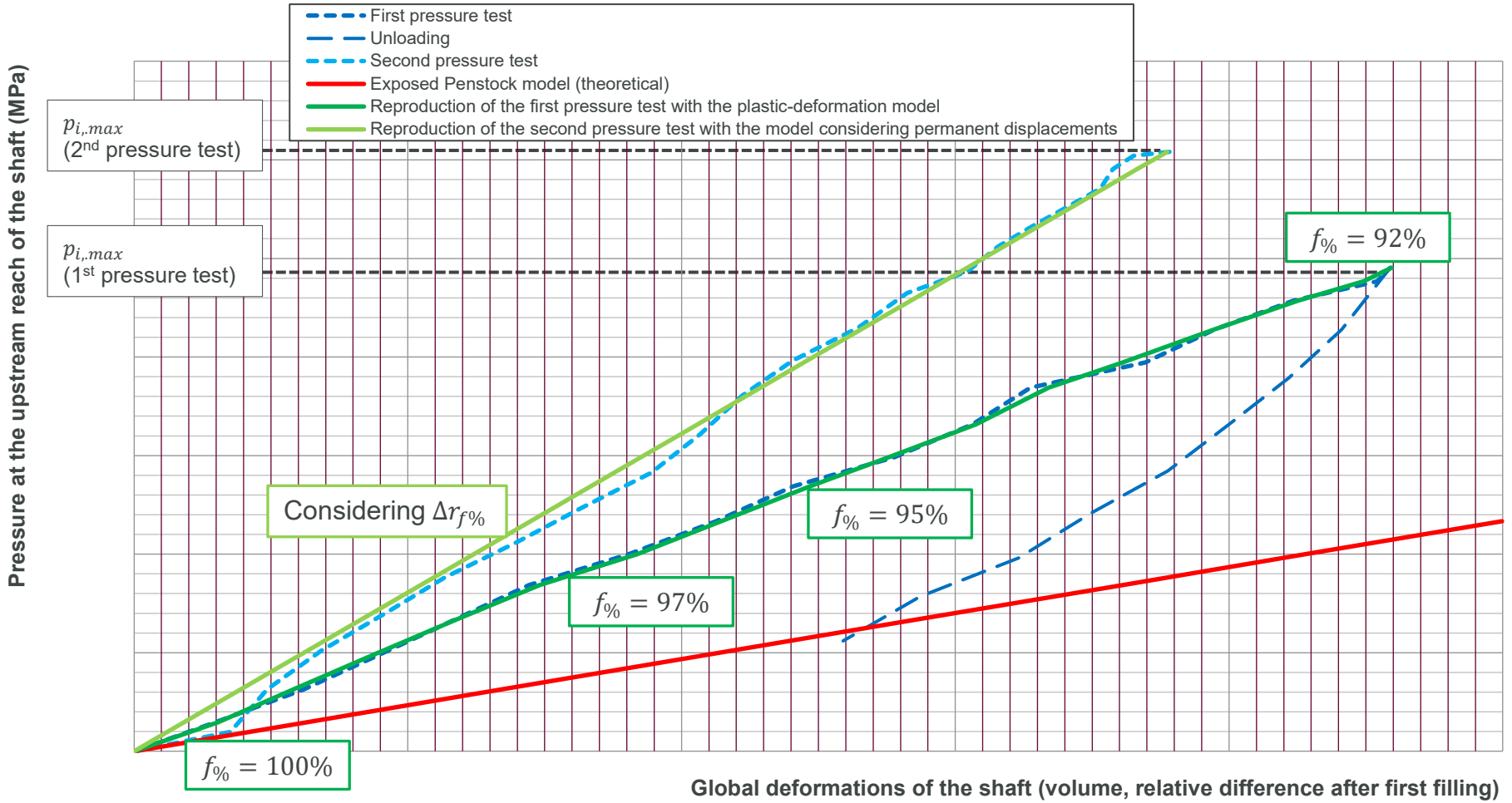

REPRODUCTION OF PRESSURE TESTS: IN THE VICINITY OF NENDAZ PLANT

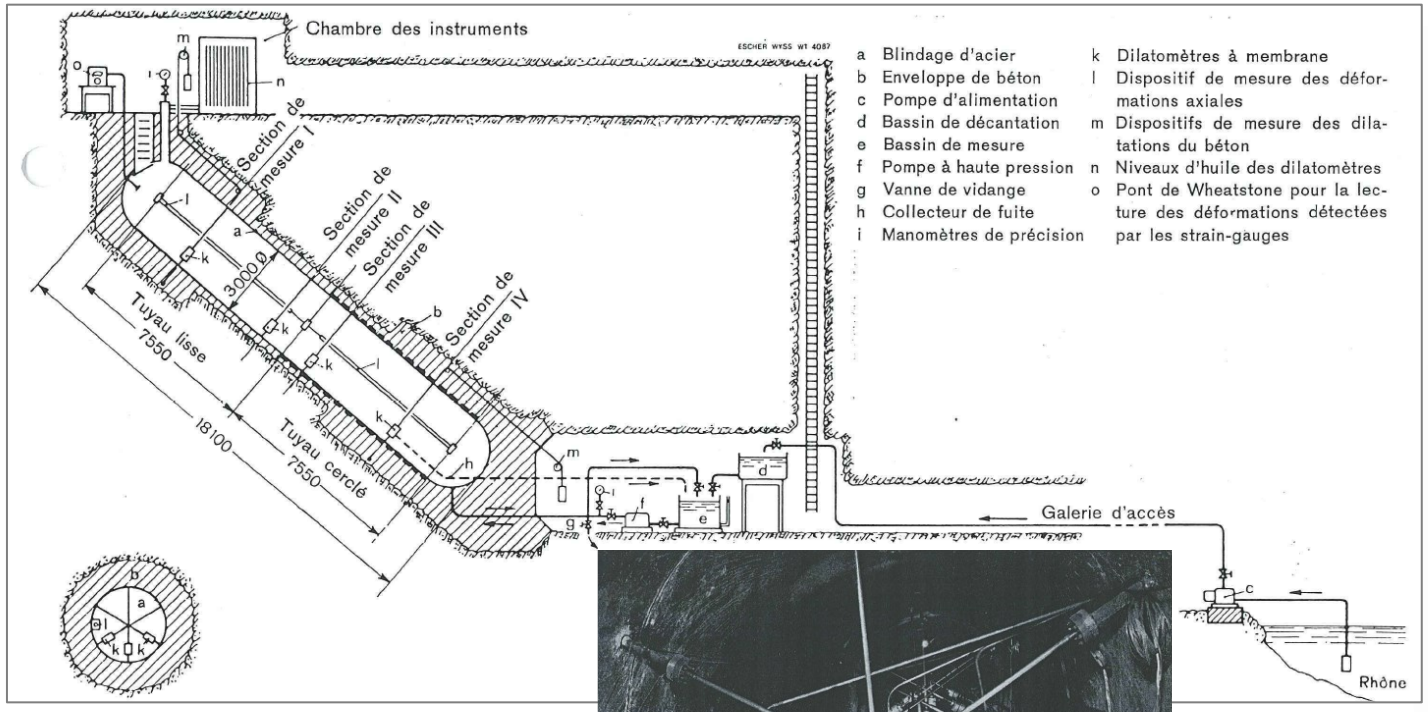

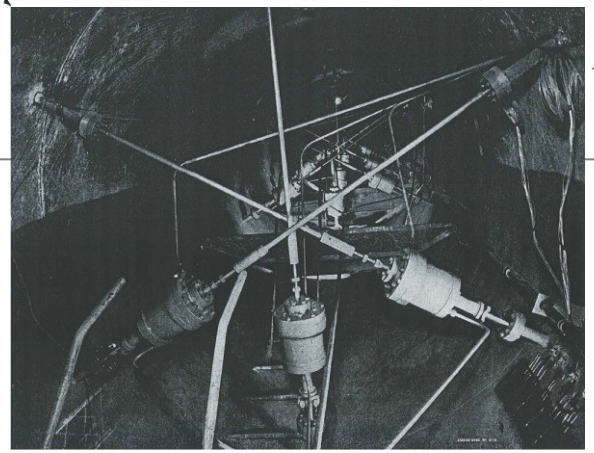

Surber (1959)

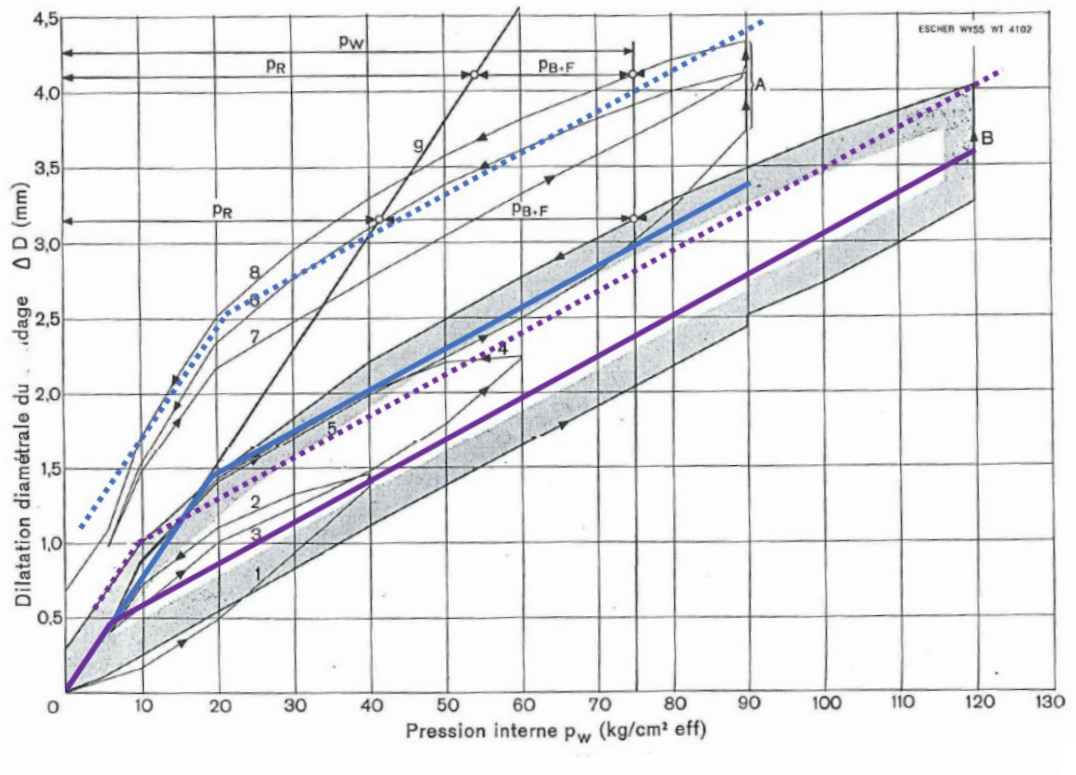

Fig. 14 Diagramme de la **déformation** selon figure 13 portée **en fonction de la pression intérieure.** La droite g figure la déformation du tuyau supposé à l'air libre sous l'effet de la pression intérieure et en l'absence d'une déformation axiale. On tire de ce diagramme les **parts de la pression intérieure supportées respectivement par la tôle et l'ensemble béton + rocher,** ceci quelle que soit cette pression intérieure. L'amélioration apportée par les injections en cours d'essai est frappante.

p_w	Pression d'eau dans le blindage	A	Première série d'essais
p_R	Part de pression supportée par le blindage	B	Deuxième série d'essais (courbe enveloppe des mesures)
p_{B+F}	Part de pression supportée par le béton et le rocher	1–8	Ordre de succession des variations de pression
g	Déformation radiale du blindage supposé libre		

SELECTED RESULTS – EXAMPLE OF STEEL LINERS AT THE GD DAM (INTAKE, HR GALLERY)

Grande Dixence SA
Technical documentation, 2015

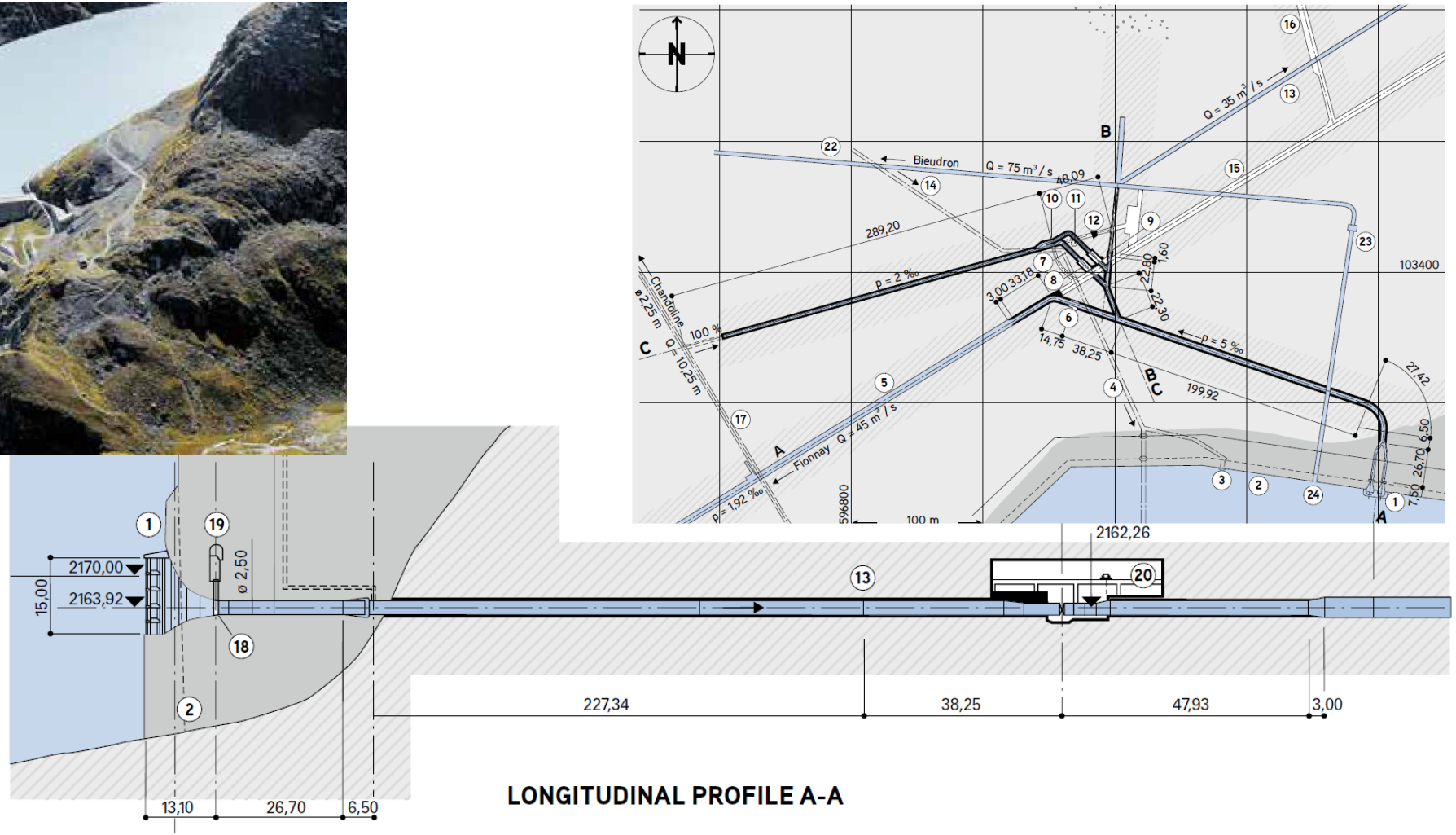

SELECTED RESULTS – DETERMINISTIC STEEL LINER WITHOUT ROCK PARTICIPATION

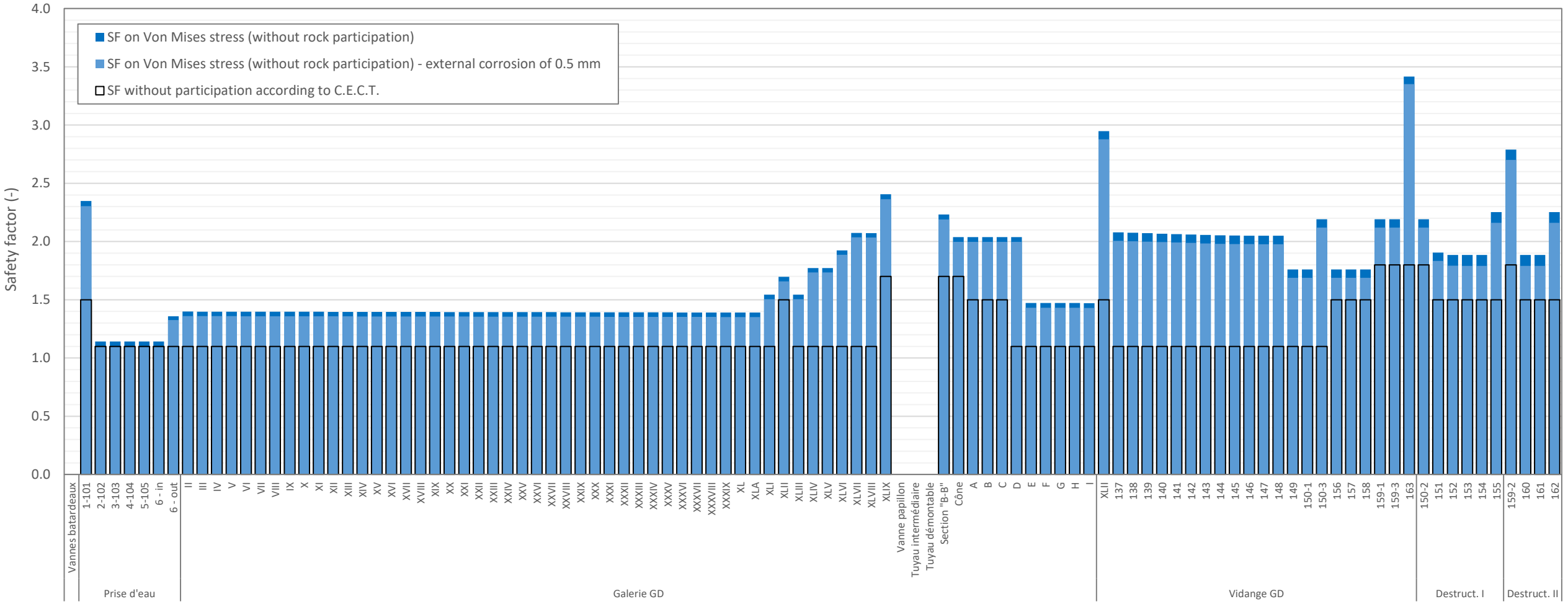

SELECTED RESULTS – DETERMINISTIC STEEL LINER WITH ROCK PARTICIPATION

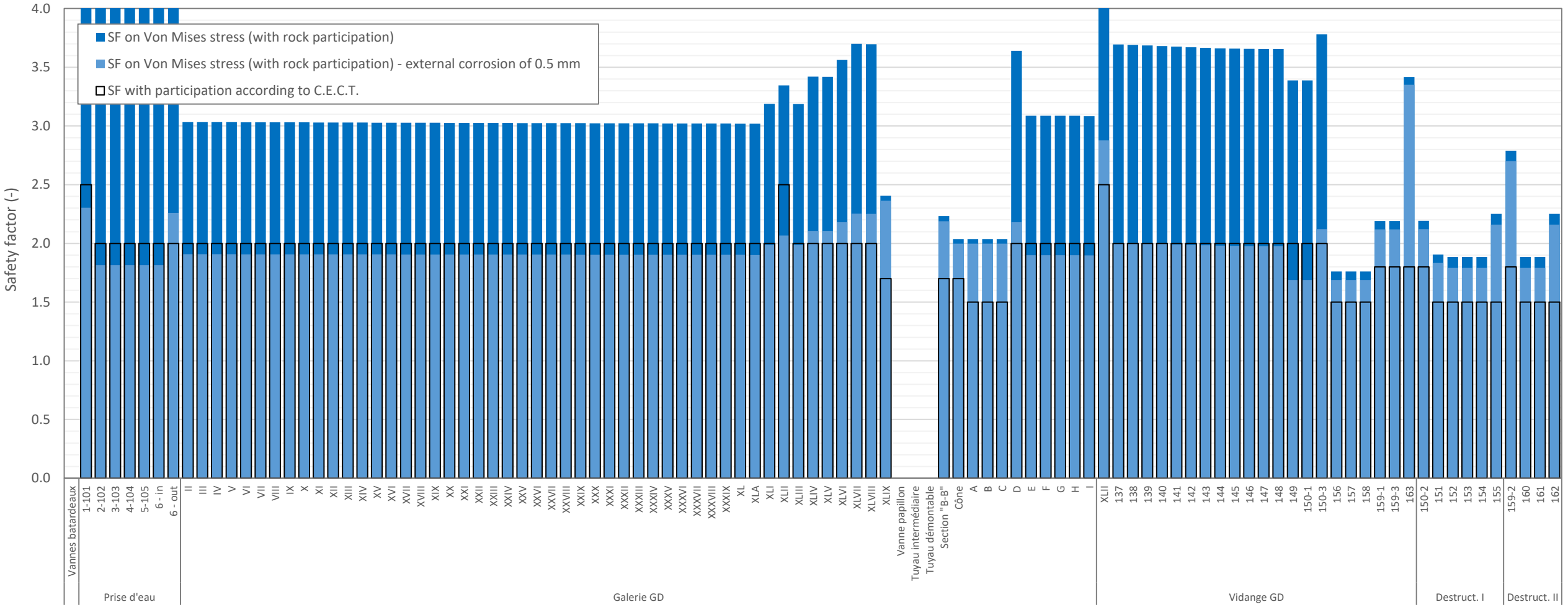

SELECTED RESULTS – DETERMINISTIC TOTAL GAP

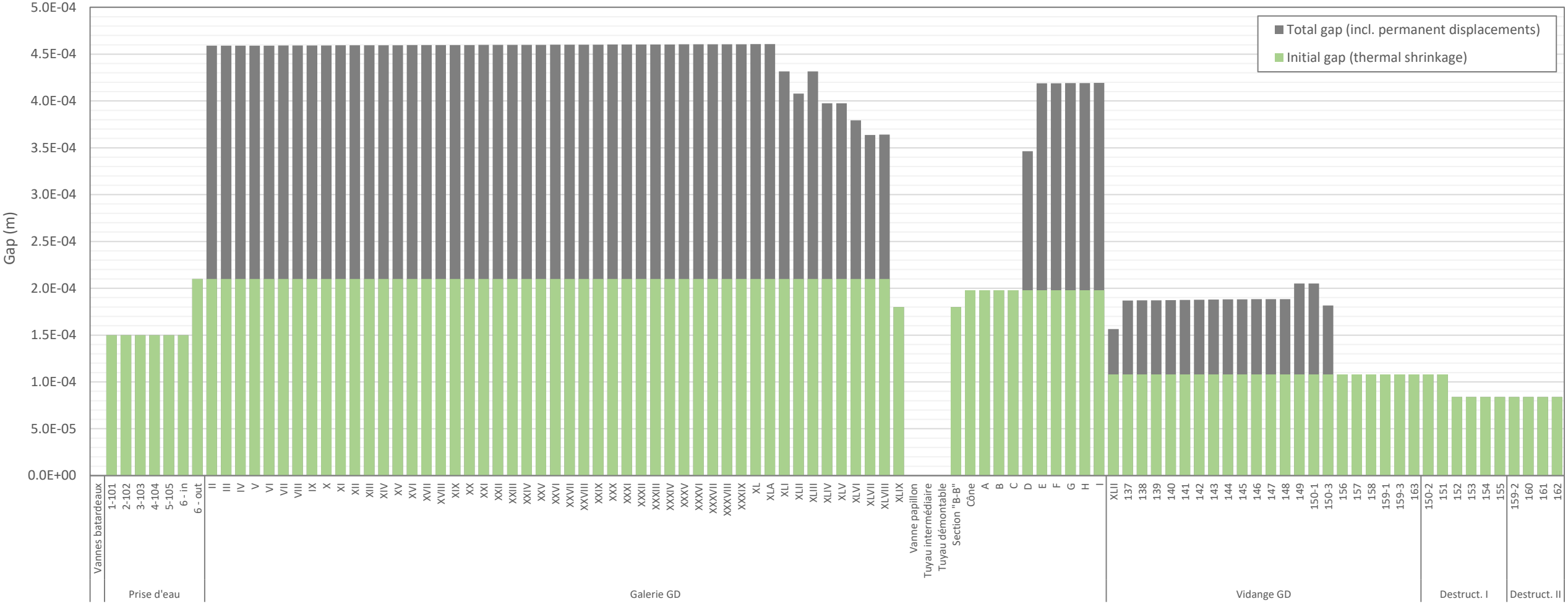

SELECTED RESULTS – DETERMINISTIC STRESSES TRANSMITTED TO ROCK

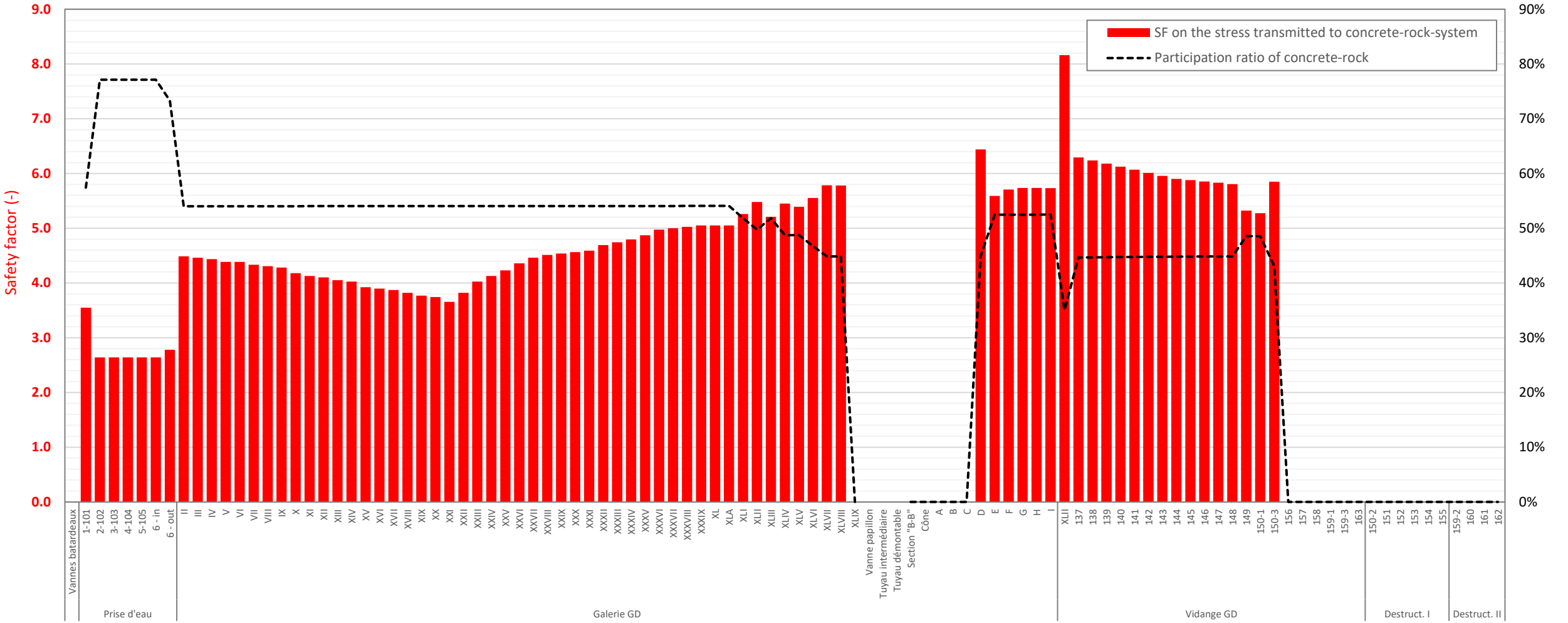

SELECTED RESULTS – STOCHASTIC MONTE CARLO SIMULATIONS (FIONNAY SHAFT)

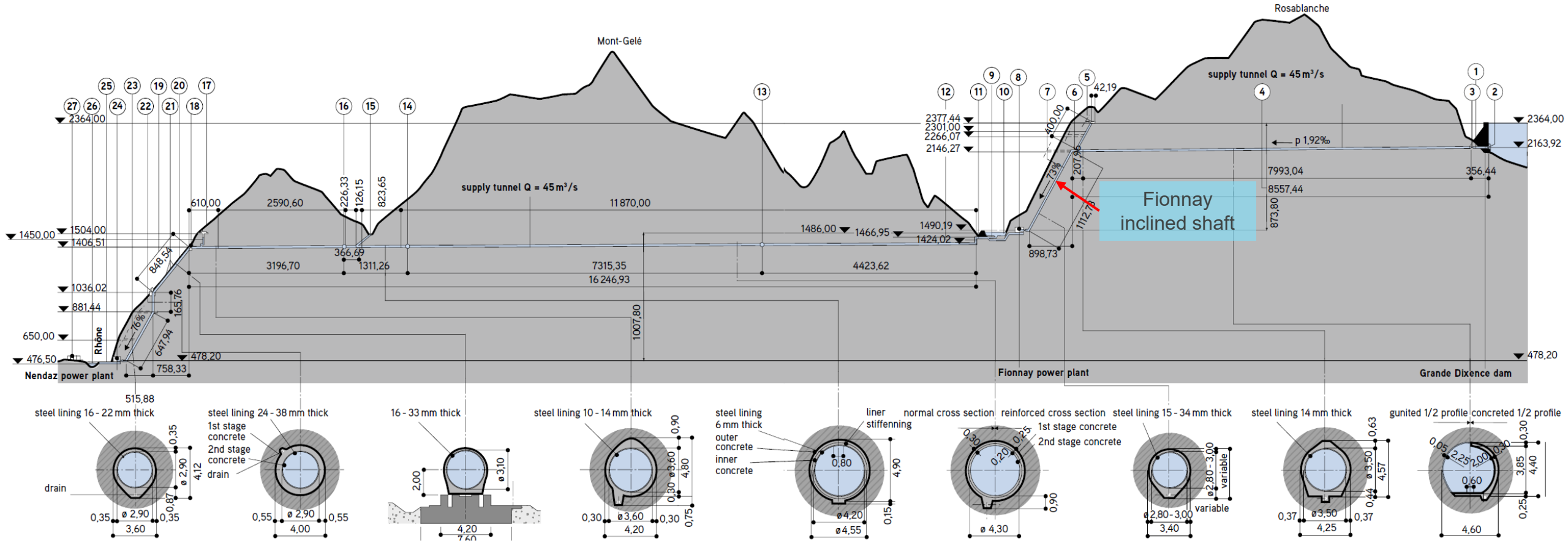

SELECTED RESULTS – STOCHASTIC MONTE CARLO SIMULATIONS (FIONNAY SHAFT)

Nom	Graphique	Fonction	Min	Moyenne	Max	Déterministe
Caractéristiques de l'acier						
Limite élastique Aldur 50	270 380	RiskLognorm(52.247;14.359;RiskShift(280);RiskStatic('ALDUR 50'!B12);RiskName("Re A50	280.00	332.25	+∞	333.5
Limite ultime Aldur 50	450 700	RiskLognorm(47.513;40.118;RiskShift(483.76);RiskStatic(D12);RiskName("Rm A50	483.76	531.27	+∞	490.5
Limite élastique Cr-Cu	310 410	RiskLognorm(55.831;13.508;RiskShift(313);RiskStatic(B12);RiskName("Re Cr-Cu	313.00	368.83	+∞	313.9
Limite ultime Cr-Cu	500 620	RiskLognorm(47.421;18.216;RiskShift(510);RiskStatic(D12);RiskName("Rm Cr-Cu	510.00	557.42	+∞	510.1
Limite élastique Aldur 42	220 320	RiskLognorm(47.801;13.684;RiskShift(225);RiskStatic(B12);RiskName("Re A42	225.00	272.80	+∞	255.1
Limite ultime Aldur 42	400 580	RiskLognorm(66.481;26.222;RiskShift(412);RiskStatic(D12);RiskName("Rm A42 [MPa]");RiskCormat(ReRmA42;2))	412.00	478.48	+∞	412.0
Caractéristiques du béton						
Module élastique du béton de remplissage	14 26	RiskTriang(15;20;25;RiskStatic(20);RiskName(B24))	15	20	25	20
Caractéristiques du rocher						
Module élastique minimum	5'000 40'000	RiskBetaGeneral(5;3.3;10000;35000;RiskStatic(15000);RiskCormat(NouvelleMatrice1;1);RiskName(B13))	10'000	25'060	35000	15'000
Module élastique maximum	20'000 50'000	RiskBetaGeneral(5;2.85;23000;45000;RiskStatic(40000);RiskCormat(NouvelleMatrice1;2);RiskName(B14))	23'000	37'013	45000	40'000
Module élastique du rocher fissuré	75% 105%	RiskUniform(0.8;1;RiskStatic(0.9);RiskName(B19))	80%	90%	100%	90%
Masse volumique	2'550 2'950	RiskTriang(2600;2700;2900;RiskStatic(2700);RiskName(B30))	2'600	2'733	2900	2'700
Résistance à la traction	-0.2 1.2	RiskTriang(0;0.5;1;RiskStatic(0.5);RiskName(B43))	0.000	0.500	1	0.500
Epaisseur du rocher fissuré	1.4 3.2	RiskUniform(1.5;3;RiskStatic(2);RiskName(B20))	1.50	2.25	3	2.00
k0	0.35 0.85	RiskUniform(0.4;0.8;RiskStatic(0.4);RiskName(C35))	0.4	0.6	0.8	0.4
Autre paramètres importants						
Variation de la température de l'acier (signe positif = refroidissement)	4 16	RiskTriang(5;10;15;RiskStatic(10);RiskName(B39))	5	10	15	10
Perte d'épaisseur du blindage par corrosion externe	-0.65 0.35	RiskTriang(0;0;0.3;RiskStatic(0);RiskName(B23))	0.00	0.10	0.3	0.00
Facteur de fluage	64% 82%	RiskTriang(0.65;0.72;0.8;RiskStatic(0.72);RiskName(B55))	0.65	0.72	0.80	0.72
Facteur d'injections	-20% 120%	RiskTriang(0;0.5;1;RiskStatic(0.8);RiskName(B60))	0.00	0.50	1.00	0.20

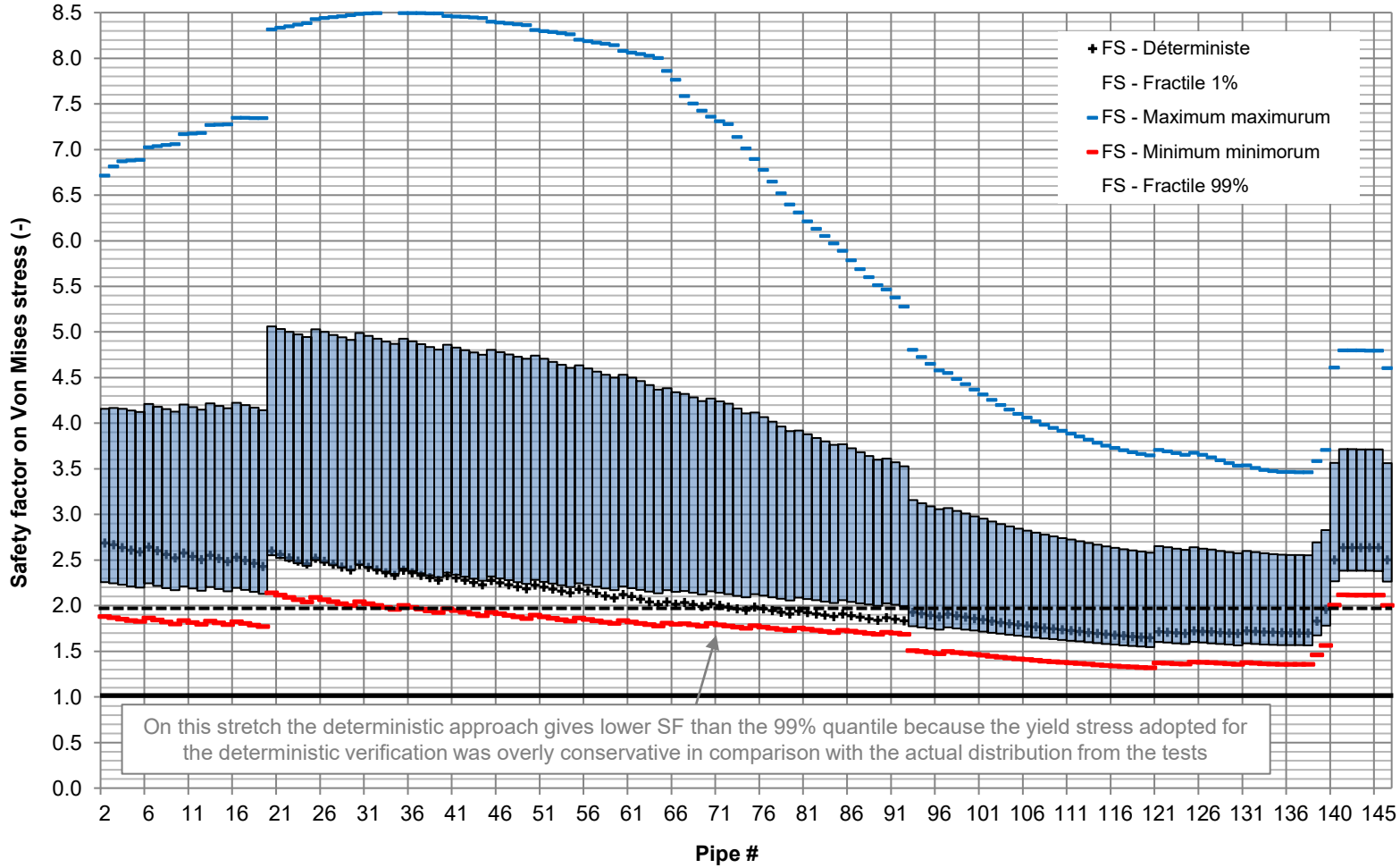

CONCLUSIONS

1. The high stakes involved in the rehab of the GD waterways have led to the development of original additions to the load sharing model for steel-lined pressure shafts and tunnels
2. The initial design assumptions have globally been verified on the entire scheme
3. Where high load sharing have been assumed beyond the recommendations of the C.E.C.T. (posterior to the construction), the assumption has been confirmed realistic
4. The project archives clearly outlined the great efforts deployed at the time of construction to ensure tightness of the backfilling, through systematic injections for the relevant parts
5. The attempt to interpret pressure tests with today's models was proven promising and allowed gaining more confidence on parameters normally subject to larger uncertainties, such as initial gap, permanent displacements and global stiffness of the multilayer system

KEY REFERENCES (LITERATURE)

[1] C.E.C.T. *Recommendations for the design, manufacture and erection of steel penstocks of welded construction for hydroelectric installations*. European Committee of boiler, vessel and pipe work manufacturers, 1980.

[2] Pachoud, A.J., Schleiss, A.J. "Stresses and displacements in steel-lined pressure tunnels and shafts in anisotropic rock under quasi-static internal water pressure". *Rock Mechanics and Rock Engineering* 49(4):1263-87, 2016.

[3] Pachoud, A.J. *Influence of geometrical imperfections and flaws at welds of steel liners on fatigue behavior of pressure tunnels and shafts in anisotropic rock*. PhD Thesis TH7305, Ecole polytechnique fédérale de Lausanne, 2017.

[4] Pachoud, A.J., Berthod, R., Manso, P.A., Schleiss, A.J. "Advanced models for stress evaluation and safety assessment in steel-lined pressure tunnels". *Hydropower & Dams (5):77-82*, 2018.

[5] Schleiss, A.J. "Design criteria applied for the lower pressure tunnel of the North Fork Stanislaus River hydroelectric project in California". *Rock Mechanics and Rock Engineering* 21(3):161-181, 1988.

[6] Surber, A. « Etude expérimentale du comportement d'un blindage de puits forcé d'une importante centrale hydro-électrique ». *Bulletin Escher Wyss* (1):3-11, 1959. (in French)

[7] Wilhelm, J. « Observation des mouvements d'une nappe d'eau souterraine entourant une galerie d'adduction d'eau en rocher ». *Schweizerische Bauzeitung* 82(2):21-28, 1964. (in French)